# The Low-temperature Crystal Structure (203 and 123 K) † and Electronic Properties of Diammonium Hexa-aquacopper(II) Disulphate: a Fluxional $CuO_6$ Chromophore

**Nathaniel W. Alcock**
*Department of Chemical and Molecular Sciences, University of Warwick, Coventry CV4 7AL*
**Mary Duggan, Angela Murray, Suresh Tyagi, and Brian J. Hathaway ***
*The Chemistry Department, University College, Cork, Ireland*
**Alan Hewat**
*Institute Max von Laue–Paul Langevin, BP156X, 38042, Grenoble, Cedex, France*

The low-temperature crystal structure of $[NH_4]_2[Cu(OH_2)_6][SO_4]_2$ (1) has been determined by *X*-ray diffraction methods at 203 and 123 K, in the monoclinic space group, $P2_1/a$. The structure changes very little with temperature, except with respect to the geometry of the $CuO_6$ chromphore which becomes more elongated rhombic octahedral with decreasing temperature (298, 203, 123 K): Cu–O(7) 2.219(5), 2.250(2), 2.278(2); Cu–O(8) 2.095(5), 2.041(2), 2.012(1); Cu–O(9) 1.961(5), 1.967(2), 1.970(1)Å. These changes are consistent with a fluxional behaviour of two 90° misaligned elongated rhombic octahedral $CuO_6$ chromophores separated by less than thermal energy. From the relative thermal populations of the lowest two wells of the potential-energy surface at the three temperatures a Boltzmann distribution, least-squares fit, enables the separation of the two wells, $\Delta E$, to be determined as 160 ± 20 $cm^{-1}$. From the temperature variations of the single-crystal *g* values (100—298 K) of (1) the $\Delta E$ value is estimated to be 168 ± 40 $cm^{-1}$, which is consistent with the crystallographic estimation of this parameter.

The interpretation [1] of the temperature variation of the e.s.r. spectrum [2] of the copper(II) doped $K_2[Zn(OH_2)_6][SO_4]_2$ system in terms of a fluxional behaviour of the $CuO_6$ chromophore between two thermally accessible elongated rhombic octahedral $CuO_6$ stereochemistries misaligned by 90° (Figure 1) raises the question of whether the $CuO_6$ chromophore stereochemistry of the corresponding concentrated copper(II) complex also involves a fluxional behaviour.[3–8] The neutron diffraction structure of $Rb_2[Cu(OH_2)_6][SO_4]_2$ at 293 and 77 K have already been determined, but showed only a slight change towards a more axially elongated rhombic octahedral stereochemistry at 77 K, consistent with only a small variation of the *g* values with decreasing temperature. As the single-crystal *g* values [2] of $[NH_4]_2[Cu(OH_2)_6][SO_4]_2$ (1) show a significant variation from 293 to 160 K, the low-temperature (l.t.) crystal structure of (1) has been determined at two temperatures, 203 and 123 K. A preliminary report [9] of the low-temperature structure (*ca.* 150 K) of (1) has been given elsewhere, involving a microdensitometer estimated set of film data, data which are considered to be less accurate than the present sets of diffractometer data.

## Experimental

*Preparation.*—Crystals of (1) were prepared by slow crystallisation of an equimolar solution of $CuSO_4 \cdot 5H_2O$ and $(NH_4)_2SO_4$ containing a few drops of sulphuric acid; the crystals were characterised by microanalysis for H, Cu, N, and S.

The crystallographic data for the two low-temperature structures of (1) and some relevant room temperature (r.t.) data are summarised in Table 1. The data were collected with a Syntex $P2_1$ four-circle diffractometer, using the LT-1 low-temperature attachment at two different temperatures. Maximum 2θ was 55°, with scan range of −0.8 to +0.95° (2θ) around the $K_{\alpha 1}$–$K_{\alpha 2}$ angles, scan speed 2—29.3° (2θ) $min^{-1}$ depending on the intensity of a 2-s pre-scan. Three standard reflections were monitored every 100 reflections; during the 123 K data set, they showed no significant variation, but during the 203 K set, some instability was apparent, and the data collection was terminated after 1 359 reflections compared with the 1 739 examined at 123 K. 1 570 and 1 302 reflections respectively, with $I/\sigma(I) > 3.0$, were retained in the refinement. Corrections were applied for Lorentz, polarisation, and absorption effects, the last using ABSCOR,[10] with maximum and minimum transmission factors 0.70 and 0.58. The copper atom was corrected for anomalous dispersion. Unit-cell dimensions and standard deviations were obtained by least-squares fit to 15 high-angle reflections.

The atomic co-ordinates for the non-hydrogen atoms, as determined in the r.t. structure.[3] were used in the initial refinement, followed by full-matrix least-squares refinement, where the function minimised was $\Sigma w(|F_o| - |F_c|)^2$ and the weight of each reflection was calculated from the expression, $w = k/[\sigma^2(F_o) + g(F_o)^2]$, see Table 1 for the final values of *k* and *g*. Calculated hydrogen positions were used initially, but ultimately refined. Complex atomic-scattering factors were employed [11] and all calculations were carried out using SHELX 76,[12] XANADU, PLUTO, and XPUB programs on an IBM 370/138 computer. Table 2 gives the final atomic co-ordinates at the temperatures of 203 and 123 K, and Table 3 the bond distances and angles. The cation numbering scheme used is that of ref. 3 and is illustrated in Figure 2, along with the 50% thermal ellipsoids of the copper and oxygen atoms for the low-temperature data at 123 K. Table 4 summarises the bond length, tetragonality and *R* value data for the $M^I_2[Cu(OH_2)_6][SO_4]_2$ ($M^I$ = K, Rb, Cs, or Tl) complexes of known crystal structure [3–8] together with $[NH_4]_2[Cu(OH_2)_6][SO_4]_2$, and Table 5 reports the corresponding root mean square displacements, $\Delta U^{\frac{1}{2}}$, along the Cu–O directions using the THMI-77 [13] thermal ellipsoid program.

*Electronic Properties.*—These were determined as previously reported.[14] The polycrystalline e.s.r. spectrum of (1) is the exchange type [14] consistent with the misalignment present in

† *Supplementary data available* (No. SUP 23750, 24 pp.): structure factors, thermal parameters, selected non-bonded distances at 203 and 123 K. See Instructions for Authors, *J. Chem. Soc., Dalton Trans.*, 1984, Issue 1, pp. xvii—xix.

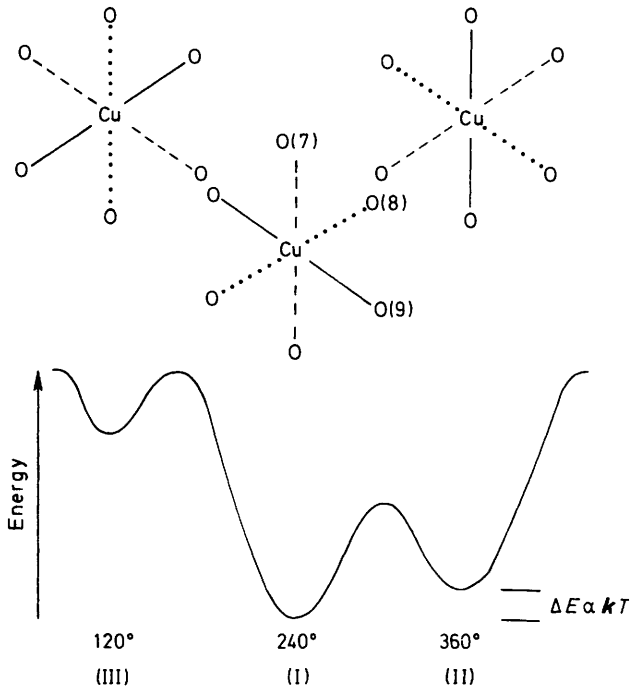


**Figure 1.** Potential-energy surface associated with the three elongated rhombic octahedral $CuO_6$ chromophores of $[NH_4]_2[Cu(OH_2)_6][SO_4]_2$, each misaligned by 90° and related to the original $C_3$ axis of the octahedral chromophore. Short (——), intermediate (• • •), and long (— — —) bonds are indicated

**Table 1.** Crystal and refinement data of $[NH_4]_2[Cu(OH_2)_6][SO_4]_2$ (1) (stoicheiometry = $H_{20}CuN_2O_{14}S_2$, $M$ = 399.67, space group = $P2_1/a$)

| | r.t. | | | |
|---|---|---|---|---|
| | X-Ray [a] | Neutron [b] | 203 K | 123 K |
| $a$/Å | 9.27 | 9.210 5(14) | 9.162(4) | 9.139(2) |
| $b$/Å | 12.44 | 12.379 5(17) | 12.326(4) | 12.278(3) |
| $c$/Å | 6.30 | 6.301 6(13) | 6.325(2) | 6.346(1) |
| β/° | 106.1 | 106.112(18) | 106.08(3) | 106.09(2) |
| $Z$ | | | 2 | 2 |
| $U$/Å$^3$ | | | 686.3(4) | 684.2(3) |
| Radiation | | | Mo-$K_\alpha$ | Mo-$K_\alpha$ |
| λ/Å | | | 0.710 69 | 0.710 69 |
| $F$(000) | | | 378.0 | 378.0 |
| μ/cm$^{-1}$ | | | 17.41 | 17.47 |
| Number of unique reflections | | | 1 359 | 1 739 |
| Number of parameters varied | | | 129 | 129 |
| $R = (\Sigma\Delta/\Sigma\lvert F_o\rvert)$ | | | 0.0350 | 0.0307 |
| $R = (\Sigma\Delta w^{\frac{1}{2}}/\Sigma\lvert F_o\rvert w^{\frac{1}{2}})$ | | | 0.0422 | 0.0393 |
| $k$ | | | 1.000 | 1.000 |
| $g$ | | | 0.004 10 | 0.002 27 |
| Maximum final shift to error ratio | | | 0.014 | 0.003 |
| Residual electron density/e Å$^{-3}$ | | | 0.39 | 0.48 |
| Number of anisotropic atoms | | | 10 | 10 |

[a] X-Ray crystallographic data from ref. 3. [b] Neutron diffraction data from ref. 4.

the unit cell [3,4] ($2\alpha$ = 10—50°) and becomes axial at the temperature of liquid nitrogen with the approximate $g$ values of 2.07 and 2.35. The single-crystal e.s.r. spectra yielded isotropic spectra along the $b$ axis ($g$ = 2.256), and in the $ac$ plane ($g_{max.}$ = 2.32 at 25° to the $a$ axis and $g_{min.}$ = 2.10), none of which corresponds to the local molecular $g$ values due to the misalignment present.[3,4] In directions between the $b$ axis and the $ac$ plane two $g$ values were observed due to the two misaligned copper(II) positions, as exchange coupling in (1) does not merge the two $g$ values from the two misaligned copper(II) centres. From the appropriate rotation, Figure 3, the three local molecular $g$ values of the r.t. structure (——) could be obtained at 2.065, 2.20, and 2.40 lying along the approximate copper to O(9), O(8), and O(7) directions respectively, which compares reasonably with those previously reported [2] of 2.071, 2.218, and 2.360. On cooling to the temperature of liquid nitrogen, $g_1$ remains unchanged, $g_2$ decreases to 2.12, and $g_3$ increases to 2.47. Figure 4 shows the variation of the single crystal $g$ values with temperature.

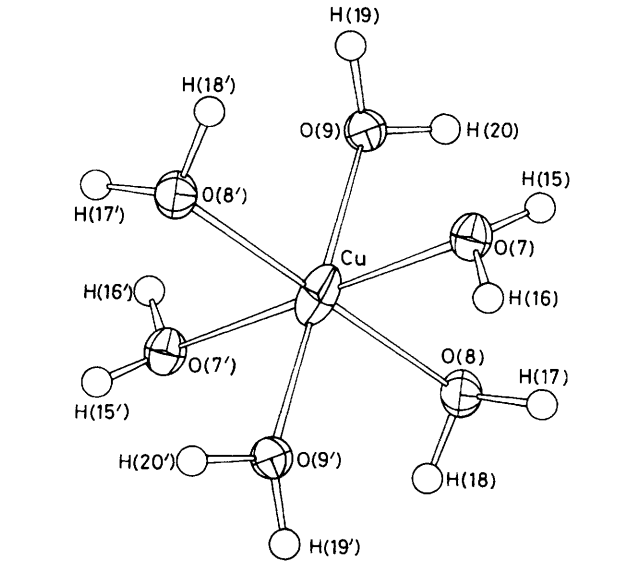


**Figure 2.** Molecular structure of the $[Cu(OH_2)_6]^{2+}$ cation, showing the thermal ellipsoids (50%) of the copper and oxygen atoms, the atom-numbering scheme, and viewed in a direction at 35° to the $b$ axis

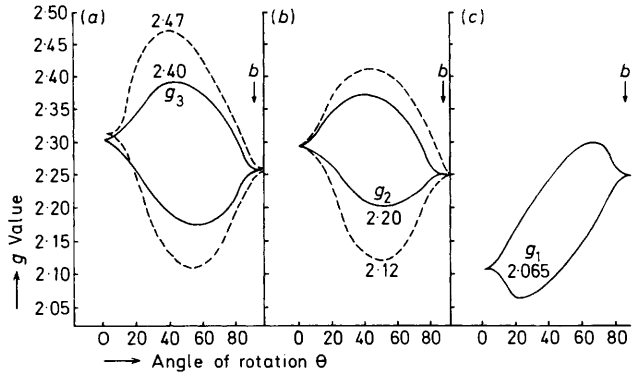


**Figure 3.** Single-crystal e.s.r. spectra of $[NH_4]_2[Cu(OH_2)_6][SO_4]_2$ measured at room temperature (——) and at the temperature of liquid nitrogen (— — —), in the plane of the $b$ axis and (*a*) the Cu–O(7) direction, (*b*) the Cu–O(8) direction, and (*c*) the Cu–O(9) direction

## Discussion

*Description of the Crystal Structures.*—The crystal structures of (1) at 203 and 123 K are basically the same as that

**Table 2.** Atomic co-ordinates ($\times 10^4$) and estimated standard deviation in parentheses

| | 203 K | | | 123 K | | |
|---|---|---|---|---|---|---|
| Atom | *X/a* | *Y/b* | *Z/c* | *X/a* | *Y/b* | *Z/c* |
| Cu | 0 000 | 0 000 | 0 000 | 0 000 | 0 000 | 0 000 |
| S | 4 137(1) | 1 379(1) | 7 461(3) | 4 175(1) | 1 365(1) | 7 457(3) |
| O(3) | 4 203(3) | 2 307(1) | 6 004(3) | 4 260(2) | 2 294(1) | 5 997(3) |
| O(4) | 5 509(3) | 740(2) | 7 827(4) | 5 553(2) | 708(1) | 7 847(3) |
| O(5) | 2 822(2) | 699(1) | 6 345(3) | 2 841(2) | 687(1) | 6 348(2) |
| O(6) | 3 953(3) | 1 796(1) | 9 557(3) | 3 992(2) | 1 795(1) | 9 544(3) |
| O(7) | 1 795(3) | 1 178(2) | 1 790(4) | 1 844(2) | 1 184(1) | 1 800(3) |
| O(8) | −1 618(2) | 1 084(2) | 289(3) | −1 586(2) | 1 083(1) | 285(2) |
| O(9) | −59(3) | −650(1) | 2 815(3) | −70(2) | −649(1) | 2 810(2) |
| N(10) | 1 373(4) | 3 459(2) | 3 596(4) | 1 399(2) | 3 436(2) | 3 588(3) |
| H(11) | 609(51) | 3 225(39) | 1 906(77) | 836(42) | 3 178(35) | 2 144(71) |
| H(12) | 2 264(59) | 3 109(36) | 3 920(69) | 2 118(39) | 3 034(30) | 3 805(54) |
| H(13) | 703(59) | 3 404(36) | 4 419(82) | 878(40) | 3 319(31) | 4 494(62) |
| H(14) | 1 572(47) | 4 066(39) | 3 701(65) | 1 649(41) | 4 099(37) | 3 948(62) |
| H(15) | 2 218(51) | 1 044(35) | 3 287(79) | 2 238(40) | 1 080(29) | 3 230(65) |
| H(16) | 2 264(80) | 1 516(59) | 1 125(113) | 2 482(43) | 1 237(28) | 1 063(61) |
| H(17) | 7 245(52) | 855(28) | 9 491(65) | 7 432(32) | 865(22) | 9 377(43) |
| H(18) | 3 704(72) | 3 338(46) | 10 256(97) | 3 698(32) | 3 168(25) | 10 067(45) |
| H(19) | 5 786(80) | 4 476(28) | 6 739(58) | 5 881(41) | 4 493(26) | 6 713(54) |
| H(20) | 4 631(31) | 3 622(31) | 6 949(66) | 4 821(34) | 3 620(26) | 6 847(52) |

**Table 3.** Bond lengths (Å) and angles (°) with estimated standard deviations in parentheses

| | 203 K | 123 K |
|---|---|---|
| Cu–O(7) | 2.250(2) | 2.278(2) |
| Cu–O(8) | 2.041(2) | 2.012(1) |
| Cu–O(9) | 1.967(2) | 1.970(1) |
| S–O(3) | 1.481(2) | 1.485(2) |
| S–O(4) | 1.447(2) | 1.458(2) |
| S–O(5) | 1.477(2) | 1.483(1) |
| S–O(6) | 1.474(2) | 1.478(2) |
| | 203 K | 123 K |
| O(7)–Cu–O(8) | 88.9(1) | 89.1(1) |
| O(7)–Cu–O(9) | 90.4(1) | 90.5(1) |
| O(8)–Cu–O(9) | 89.0(1) | 88.9(1) |
| O(3)–S–O(4) | 109.7(1) | 109.8(1) |
| O(3)–S–O(5) | 108.1(1) | 108.2(1) |
| O(3)–S–O(6) | 109.0(1) | 108.8(1) |
| O(4)–S–O(5) | 109.0(1) | 109.2(1) |
| O(4)–S–O(6) | 110.9(1) | 110.6(1) |
| O(5)–S–O(6) | 110.2(1) | 110.1(1) |

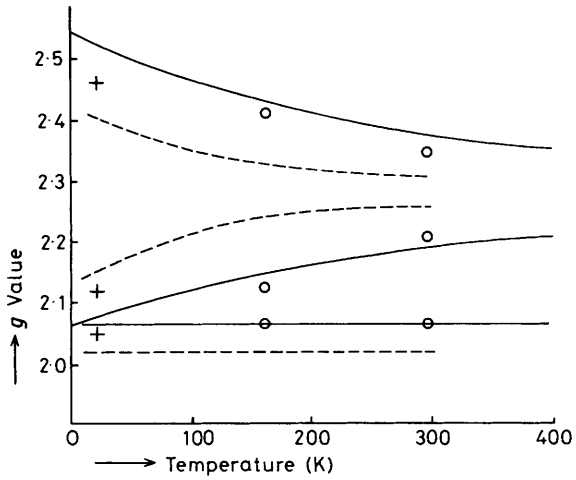


**Figure 4.** Temperature variation of the single-crystal e.s.r. spectra of $[NH_4]_2[Cu(OH_2)_6][SO_4]_2$ at *X*-band (——) and at *Q*-band (O). The single-crystal *g* values of copper doped $[NH_4]_2[Zn(OH_2)_6][SO_4]_2$ (+) and the polycrystalline e.s.r. spectrum of copper doped $K_2[Cu(OH_2)_6][SO_4]_2$ (— — —) are also shown

reported at room temperature,[3,4] with discrete $NH_4^+$ and $[Cu(OH_2)_6]^{2+}$ cations and $SO_4^{2-}$ anions connected by a network of hydrogen bonds (see Supplementary Publication), showing little difference between r.t. and l.t. (see later). Each water molecule forms two hydrogen bonds with the oxygen of the sulphate anion, which is also hydrogen bonded to the ammonium cation. The close approach of the two O(9) atoms of 3.14 Å at l.t., across the centre of symmetry at $0,0,\frac{1}{2}$, is also present in the r.t. structure.

There are no significant differences between the r.t. and l.t. structures, in the bond lengths and bond angles of the tetrahedral ammonium cations and sulphate anions, or in the bond angles of the centrosymmetric $CuO_6$ chromophore, but there are significant differences in the three copper–oxygen bond lengths. The Cu–O(7) bond distance shows a significant increase with decreasing temperature, the Cu–O(8) bond distance significantly decreases, and the Cu–O(9) bond distance shows a very slight increase. These results are illustrated graphically in Figure 5. Taken together these changes reflect an increase in the elongation of the rhombic octahedral $CuO_6$ chromophore with decrease in temperature and a reduction in the rhombic component to a more nearly axial structure. The $CuO_6$ chromophore is clearly rhombic octahedral at r.t. with a tetragonality, *T* (defined as the mean in-plane Cu–O bond length divided by the mean out-of-plane bond length, $R_S/R_L$) of $<1.00$, consistent with the elongated rhombic octahedral stereochemistry present, Table 4. The structure of (1) has been determined at r.t. (*ca.* 298 K) by both *X*-ray and neutron diffraction techniques, with the latter having a slightly lower *R* value, and hence should be accepted as the more accurate determination. There are significant differences in the two r.t. structures, Table 4(*a*), which result in the significantly different tetragonalities of 0.914 and 0.904 respectively, suggesting that either there are significant differences in the two structure determination techniques or that the two determinations were carried out at different temperatures (see later). If the tetragonalities (*T*) of the r.t.

**Table 4.** Bond length and tetragonality ($T$) data, estimated $\Delta E$ ($cm^{-1}$), and ground state thermal population values $n_1$ (%) for $[NH_4]_2[Cu(OH_2)_6][SO_4]_2$ and $M^I_2[Cu(OH_2)_6][SO_4]_2$ complexes

(*a*) $[NH_4]_2[Cu(OH_2)_6][SO_4]_2$

| | r.t.[a] | r.t.[b] | 203 K | 123 K |
|---|---|---|---|---|
| Cu–O(7) | 2.219(5) | 2.230(1) | 2.250(2) | 2.278(2) |
| Cu–O(8) | 2.095(5) | 2.072(1) | 2.041(2) | 2.012(1) |
| Cu–O(9) | 1.961(5) | 1.966(1) | 1.967(2) | 1.970(1) |
| $T$ | 0.914 | 0.904 | 0.891 | 0.874 |
| $R$ value | 0.060 | 0.0548 | 0.0350 | 0.0307 |
| $\Delta E$ | 160 | 175 | 160 | 160 |
| $n_1$ | 66 | 70 | 78 | 86 |

(*b*) $M^I_2[Cu(OH_2)_6][SO_4]_2$

| $M^I$ | K[b] | Rb[b] | Cs[b] | Tl[b] | Rb (77 K)[b] |
|---|---|---|---|---|---|
| Cu–O(8)[c] | 2.278(2) | 2.307(3) | 2.315(5) | 2.317(5) | 2.317(5) |
| Cu–O(7)[c] | 2.069(3) | 2.031(3) | 2.004(4) | 2.017(4) | 2.000(5) |
| Cu–O(9) | 1.943(3) | 1.957(3) | 1.966(5) | 1.957(5) | 1.978(5) |
| $T$ | 0.881 | 0.864 | 0.858 | 0.858 | 0.858 |
| $R$ value | 0.052 | 0.069 | 0.043 | 0.064 | 0.075 |
| $\Delta E$ | 267 | 402 | 510 | 470 | 402 |
| $n_1$ | 78 | 87 | 92 | 91 | — |

[a] *X*-Ray data, ref. 3. [b] Neutron diffraction data, ref. 4. [c] In all the alkali metal Tutton salts[6,7] the long Cu–O bond is to O(8) rather than to O(7) as in the $NH_4^+$ salt.

**Table 5.** Root mean square displacements, $\Delta U^{\frac{1}{2}}$, along the Cu–O directions (Å) for $[NH_4]_2[Cu(OH_2)_6][SO_4]_2$ and $M^I_2[Cu(OH_2)_6][SO_4]_2$ ($M^I$ = K, Rb, Tl, or Cs) complexes

| | $NH_4^+$[a] | $NH_4^+$[b] | $NH_4^+$[b] | K[a] | Rb[a] | Tl[a] | Cs[a] |
|---|---|---|---|---|---|---|---|
| Temp./K | 298 | 203 | 123 | 298 | 298 | 298 | 298 |
| Cu–O(7)[c] | 0.125 | 0.141 | 0.123 | 0.104 | 0.084 | 0.096 | 0.099 |
| Cu–O(8)[c] | 0.112 | 0.132 | 0.122 | 0.104 | 0.080 | 0.092 | 0.088 |
| Cu–O(9) | 0.062 | 0.107 | 0.106 | 0.066 | 0.069 | 0.062 | 0.057 |
| $T$ | 0.914 | 0.891 | 0.874 | 0.881 | 0.864 | 0.858 | 0.858 |

[a] Neutron diffraction data. [b] *X*-Ray data. [c] For alkali metal salts O(7) and O(8) interchanged.

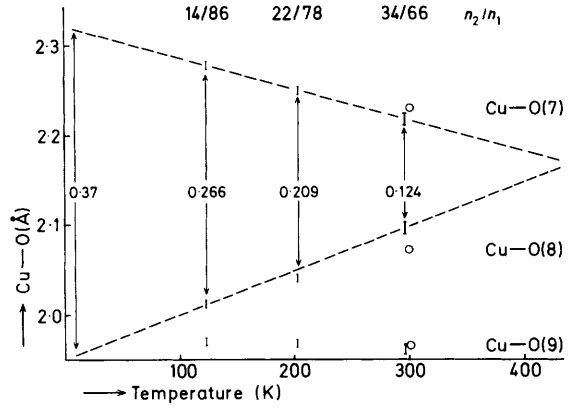


**Figure 5.** Cu–O distances (Å) as a function of temperature for $[NH_4]_2[Cu(OH_2)_6][SO_4]_2$ for (*a*) *X*-ray data (I) and (*b*) neutron diffraction data (O). Values (Å) of [Cu–O(7)] – [Cu–O(8)] are also indicated ($n_1$ = ground state population, $n_2$ = upper state population)

structures are plotted against the axial bond lengths ($R_L$) there is a reasonable correlation between the r.t. data and the two sets of l.t. structural data, Figure 6. This suggests that both of the r.t. data sets are valid and should be retained. If the observed Cu–O bond distances are plotted against the absolute temperature of these structure determinations, Figure 5, there is a reasonable correlation between the data for the three sets of *X*-ray diffraction data but the neutron diffraction data set is significantly different, suggesting that the latter was measured at a significantly lower temperature.

Nevertheless, all four sets of data demonstrate a clear decrease of the tetragonality with decreasing temperatures as was first suggested[9] using a set of l.t. film data. However, these data were limited to 629 reflections and yielded a relatively high $R$ value of 0.0906; it is clearly less accurate than any of the above four sets of data and as the tetragonality of 0.865 lies significantly away from the correlation of Figure 6, this data set will not be considered further.

Table 4(*b*) summarises the Cu–O bond distances, the tetragonalities, and the $R$ values for the other $M^I_2[Cu(OH_2)_6][SO_4]_2$ complexes[5–8] of known crystal structure using *X*-ray and neutron diffraction data. All four r.t. structures involve an elongated rhombic octahedral $CuO_6$ chromophore stereochemistry with tetragonalities in the range 0.881—0.858.

The l.t. data for the rubidium Tutton salt,[6] Table 4(*b*), shows only a slight change with temperature with a hardly significant decrease in the tetragonality from 0.864 to 0.858. This is a value that coincides with the r.t. data for the caesium Tutton salt[7] and this fits in with the r.t. correlation of Figure 6, a behaviour in contrast to the 203 and 123 K data for (1), which show a significant divergence from the linear correlation r.t. data of Figure 6.

*A Fluxional Model for the* $CuO_6$ *Chromophore.*—The marked temperature variation of the tetragonality (Table 4) of the elongated rhombic octahedral $CuO_6$ chromophore of (1) may

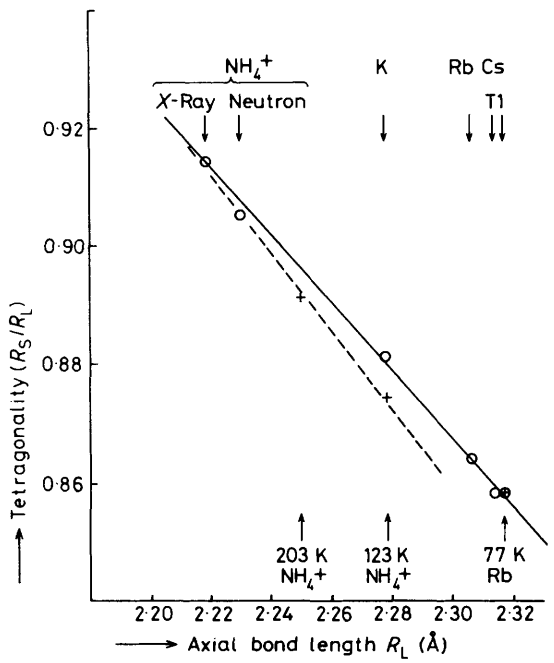


**Figure 6.** Tetragonality ($R_S/R_L$) *versus* axial bond length at room temperature (○) and low temperature (+) for $[NH_4]_2[Cu(OH_2)_6][SO_4]_2$ and $M^I_2[Cu(OH_2)_6][SO_4]_2$ ($M^I$ = K, Rb, Cs, or Tl): correlation of r.t. (——) and l.t. (— — —) data

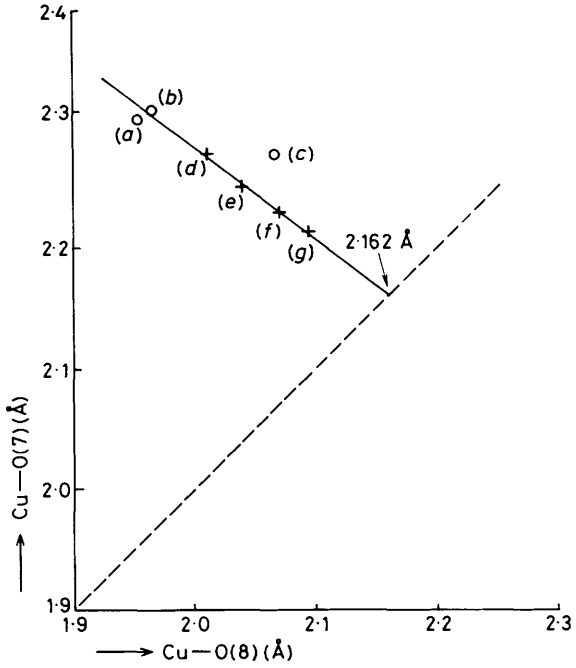


**Figure 7.** Cu–O(7) distance *versus* Cu–O(8) distance for $M^I_2[Cu(OH_2)_6][SO_4]_2$ [$M^I$ = Rb (*a*), Cs (*b*), or K (*c*)] at room temperature and $[NH_4]_2[Cu(OH_2)_6][SO_4]_2$ at 123 (*d*), 203 (*e*), 298 (neutron) (*f*), and 298 K (*X*-ray) (*g*)

be rationalised in terms of a fluxional model [1,15] involving a potential energy surface of *three* possible elongated tetragonal octahedral $CuO_6$ chromophores (Figure 1). The lowest potential energy well (I) corresponds with the elongation along Cu–O(7) bond, the next lowest (II) to elongation along Cu–O(8), and the highest (III) to elongation along Cu–O(9). At a particular temperature the observed structure will be an average of the three possible orientations weighted according to their relative thermal populations. In the r.t. structure of the caesium Tutton salt,[7] only the lowest potential well (I) is occupied and with $\Delta E \gg kT$ ($\approx 200$ cm$^{-1}$) the intermediate (II) and highest (III) potential wells are unoccupied, resulting in a non-temperature-variable elongated rhombic octahedral stereochemistry with a relatively low tetragonality, $T = 0.858$. In the rubidium Tutton salt [6] the tetragonality is slightly higher at 0.864, but reduces to 0.858 at the temperature of liquid nitrogen, suggesting that at r.t. there is a small but significant thermal population of the intermediate potential well (II) and implies that $\Delta E$ is lower than in the Cs salt and nearer to $kT$. In the potassium and especially the ammonium Tutton salt there is even greater thermal population of well (II) at r.t. and the tetragonalities increase to 0.881 and 0.914 respectively [for the *X*-ray data for (I)], and suggest that $\Delta E$ is probably less than $kT$, with significant thermal population of well (II). The observed crystal structures will then correspond to a weighted mean of the two misaligned (90°) elongated tetragonal octahedral chromophores of wells (I) and (II), proportional to their relative thermal populations. The effect of lowering the temperature on (I) will be to depopulate the higher energy well (II) (but not to zero), and increase the thermal population of well (I); this will result in the apparent elongation of the observed $CuO_6$ chromphore and a corresponding decrease in the observed tetragonalities from 0.914 to 0.874 at 123 K. As the latter is significantly higher than the r.t. tetragonality of the caesium Tutton salt [7] it suggests that there is still a significant thermal population of well (II), even at 123 K, and hence of fluxional behaviour even at this low temperature in (I). This suggestion is supported by some preliminary data [16] for the deuteriated form of (I), namely, $[ND_4]_2[Cu(OD_2)_6][SO_4]_2$ obtained by profile analysis [17] of the powder neutron diffraction spectrum measured at 5 K, which yielded Cu–O distances of O(7) 2.304(6), O(8) 2.011(4), and O(9) 1.951(4) Å, respectively. While these Cu–O distances may be less certain than those obtained for the single-crystal data (Table 4), they clearly indicate that at the lower temperature of 5 K, there is a further decrease in tetragonality to 0.860 very close in value to that of 0.858 observed [6,7] in the Cs and l.t. Rb structures, Table 4. These powder data, although measured on the deuteriated form of (I), strongly suggest that the temperature variation of (I) may reasonably be extrapolated to 0 K, at which temperature the structure corresponds to the underlying static stereochemistry of well (I) (Figure 1), a structure that equates with the r.t. structure of the Cs salt.

If the structural data for (I) are plotted as in Figure 7 then a linear correlation is obtained (correlation coefficient −0.9998) further supporting the fluxional description of the $CuO_6$ chromophore of (I). If the corresponding data for Rb and Cs are plotted these points lie very close to the linear correlation of the data for (I) and further support the suggestion that the r.t. structure of the Cs salt is a fair representation of the underlying static stereochemistry of (I), and may be used [1] to estimate the relative thermal populations of wells (I) and (II), namely $n_1$ and $n_2$, which may then be used to estimate the energy difference ($\Delta E$) using a Boltzmann distribution, $\ln(n_1/n_2) = \Delta E/RT$, for the data of (I).

*Calculation of* $\Delta E$.—Following ref. 1, the Cu–O distances may be expressed by equations (1) and (2), where $K$ is the

$$\text{Cu–O(7)} = 2.30\,\frac{K}{K+1} + 2.00\,\frac{1}{K+1} \qquad (1)$$

$$\text{Cu–O(8)} = 2.00\,\frac{K}{K+1} + 2.30\,\frac{1}{K+1} \qquad (2)$$

**Table 6.** Estimates of the average Cu–O distance, $d_0$, and the Jahn–Teller radius, $R_{J.T.} = \sum_{i=1}^{6} (\Delta d_i^2)^{\frac{1}{2}}$ *

(*a*) Room temperature

| | $NH_4^+$ [a] | $NH_4^+$ [b] | K | Rb | Cs | Tl |
|---|---|---|---|---|---|---|
| $d_0$/Å | 2.092 | 2.089 | 2.097 | 2.098 | 2.095 | 2.097 |
| $\Sigma\Delta d_i^2$/Å$^2$ | 0.0669 | 0.0706 | 0.1145 | 0.1361 | 0.1466 | 0.1488 |
| $R_{J.T.}$/Å | 0.259 | 0.266 | 0.388 | 0.369 | 0.383 | 0.385 |

(*b*) Low temperature

| | $NH_4^+$ | | | Rb |
|---|---|---|---|---|
| | 298 | 203 | 123 | 77 |
| $d_0$/Å | 2.092 | 2.086 | 2.087 | 2.098 |
| $\Sigma\Delta d_i^2$/Å$^2$ | 0.0669 | 0.0862 | 0.1116 | 0.1466 |
| $R_{J.T.}$/.Å | 0.259 | 0.294 | 0.334 | 0.383 |

* Ligand oxygen atoms are numbered $O_i$ ($i$ = 1—6); $d_i$ = Cu − $O_i$ distance; $\Delta d_i = d_0 - d_i$.

relative thermal population, $n_1/n_2$, and may be re-expressed in a more convenient form,[18] $n_1/n_2 = (\delta^m + \delta)/(\delta^m - \delta)$, where $\delta$ is the difference, [Cu–O(7)] − [Cu–O(8)], observed at a given temperature and $\delta^m$ is the maximum $\delta$ extrapolated to 0 K. Assuming various reasonable values of $\delta^m$ (0.3—0.4 Å), it is then possible to calculate $n_1/n_2$ values at 298, 203, and 123 K. If the data are plotted as ln $(n_1/n_2)$ *versus* $T^{-1}$ a linear plot passing through the origin should be obtained. If a least-squares analysis (including the origin) is carried out, the best $\delta^m$ value of 0.37 Å (correlation coefficient = 0.990) is obtained, and yields a $\Delta E$ value of 160 ± 20 cm$^{-1}$ (Table 5), below thermal energy and yielding the relative thermal population of Table 4(*a*). While the plot of ln $(n_1/n)_2$ *versus* $T^{-1}$ is not ideal, the point that shows the maximum divergence is for the 203 K data collection, which is the least accurate of the two l.t. data sets, as significantly fewer reflections were estimated (Table 1). If this point is omitted an improved correlation is obtained passing near the origin, but then reduces the data to only two points, which is not justified. Equally significant for all the data, it is the r.t. point (*X*-ray data) that shows the least divergence from the linear correlation, and justifies the assumption in the expressions for Cu–O(7) and Cu–O(8) that only two potential wells (I) and (II) are occupied at r.t. If this were not the case and well (III) were thermally populated at r.t., it would be the r.t. point that should show the greatest divergence from a linear plot. The observation that the Cu–O(9) distance shows only a very small increase with decreasing temperature, is consistent with this assumption, as the Cu–O(9) distance would be expected to decrease with decreasing temperature if the thermal population of well (III) were significant, especially at r.t.

The ability to estimate a $\Delta E$ value of 160 cm$^{-1}$ for the fluxional behaviour of the $[Cu(OH_2)_6]^{2+}$ ion in (1) from temperature-variable crystallographic data is most important in demonstrating that the energy differences of the potential energy surface of Figure 1 can be obtained from crystallographic data.[19] The use of crystallographic data to estimate $\Delta E$ values (75 cm$^{-1}$) has been previously used [18,20] for the fluxional $CuN_4O_2$ chromophore in $[Cu(bipy)_2(ONO)][NO_3]$ (bipy = 2,2′-bipyridyl) using single-crystal data down to 20 K. A value for $\Delta E$ of 75 cm$^{-1}$ for the $[Cu(OH_2)_6]^{2+}$ ion has been previously obtained [1] from the temperature-variable $g$ values for this cation doped in the diamagnetic host lattice of $K_2[Zn(OH_2)_6][SO_4]_2$. While there is a clear numerical difference between the two estimates, two entirely different physical techniques were used. Equally, the present data relate to the $CuO_6$ chromophore in a concentrated copper(II) complex, the latter relate to the $CuO_6$ chromophore doped in a zinc(II) host lattice,[21] which although isomorphous, is not isostructural with the copper(II) complex [3,4] and the co-operative Jahn–Teller Effect [22] may operate. In addition, although Tutton salts are involved in both estimates, the present data refer to the ammonium complex, while the e.s.r. data [1] refer to the potassium salt and the 'plasticity effect' [23] alone may account for the significantly different values for $\Delta E$ that are obtained.

Using the above estimated value for $\delta^m$ of 0.37 Å for (1), it is then possible to estimate values of $n_1$ and $\Delta E$ from the crystallographic data, for the K, Rb, Cs, and Tl Tutton salts as shown in Table 4(*b*). As the crystallographic data suggest, the thermal populations of well (II) are all significantly less than for (1) and decrease in the sequence K to Tl, with corresponding increases in the $\Delta E$ values. Both the data of Table 4(*b*) and Figure 6 imply that the extent of fluxional behaviour in this series of Tutton salts decreases with the atomic size or weight of the cation present and suggests that the energy required to promote the $CuO_6$ through an energy of $\Delta E$ is a function of the ability of the lattice to relax and allow the fluxional change. The larger the cation the more energy is required to allow the change in elongation direction required by the changes of Figure 1, which must in part be controlled by the hydrogen bonding network of the Tutton salt lattice (see ref. 16).

*Estimates of the Jahn–Teller Radius.*—The data of Table 4 enable an estimate [24] to be made for the $CuO_6$ chromophore of the average Cu–O distance, $d_0$, and the Jahn–Teller radius,[24] $R_{J.T.} = \sum_{i=1}^{6} (\Delta d_i^2)^{\frac{1}{2}}$, for a number of static and fluxional $CuO_6$ systems. The $d_0$ values are essentially constant, 2.093 ± 0.005 Å, as previously suggested [24] for some $CuN_6$ chromophores, whether or not the $CuO_6$ chromophores are fluxional or static. The $R_{J.T.}$ values are clearly not constant, but are significantly lower for the fluxional systems, 0.25—0.35 Å, but tend to a maximum value of 0.38 Å for static systems, Table 6. This result contrasts with the constant value of 0.32 ± 0.03 Å previously suggested [24] for the $CuN_6$ chromophore in both static and dynamic systems covering a wide range of ligands. Why the $CuO_6$ chromophores do not fit the constant $R_{J.T.}$ value previously suggested is not clear, but the range of $CuO_6$ chromophores is limited to the $[Cu(OH_2)_6]^{2+}$ cation.

*E.S.R. Spectra.*—The observation of an exchange type e.s.r. spectrum [14] for (1) is consistent with the misalignment of the $CuO_6$ chromophores. It is then surprising that the local molecular $g$ values of the two non-equivalent orientations are

so clearly resolved in the single-crystal e.s.r. spectra, Figure 3(*a*)—(*c*). With a copper–copper separation [3,4] in the unit cell of 6.6 Å, the absence of exchange coupling to merge the $g$ values, as normally observed, is not understood, and it was equally fortuitous that copper hyperfine structure [14] was not observed on any of the $g$ values to complicate the interpretation of the spectra. The angular variation of the single-crystal $g$ values, Figure 3, is then consistent with a rhombic set of $g$ values (2.065, 2.20, and 2.40) lying approximately parallel to the Cu–O(9), Cu–O(8), and Cu–O(7) bond directions,[3,4] respectively. The $R_{e.s.r.}$ value [14] [$= (g_2 - g_1)/(g_3 - g_2)$] of 0.675 is then consistent with the elongated rhombic octahedral $CuO_6$ chromophore stereochemistry with the relatively high tetragonality of 0.914. The temperature variation of the $g$ values (Figure 4), 2.10, 2.12, and 2.47, yields a significantly lower $R_{e.s.r.}$ value of 0.06 consistent with the lower tetragonality of the 123 K structure of 0.874. This pattern of temperature variation of the $g$ values, $g_3$ increasing and $g_2$ decreasing with decreasing temperature, while $g_1$ remains temperature invariant, was first established [1] to explain the fluxional behaviour of the copper(II) doped $K_2[Zn(OH_2)_6][SO_4]_2$ system and more recently, the copper(II) doped $[Zn(dien)_2]X_2$ (dien = diethylenetriamine) [25] and zinc(II) bis(pyridine-3-sulphonate) tetrahydrate [26] systems. The present l.t. crystallographic data for (1) represent the first crystallographic evidence to support the suggested temperature variation of the six-co-ordinate $CuL_6$ chromophore structures, as postulated by the temperature-variable e.s.r. data for any of these systems.

While the temperature variations of the single-crystal $g$ values, Figure 4, are less certain than that of the crystallographic data, Figure 5, they establish a clear temperature variation of $g_2$ and $g_3$ with a small but definite variation in $g_1$. Figure 4 also shows the temperature variation of the copper-doped $K_2[Zn(OH_2)_6][SO_4]_2$ system [1] down to near helium temperature and the single-crystal $g$ values for (1) previously recorded at 293 and 160 K. The temperature variation of the copper-doped potassium Tutton salt is clearly different from either of the single-crystal $g$ value measurements for (1) and clearly rules out any expectation that the $\Delta E$ values should be the same in the two systems. There is reasonable agreement between the two single-crystal $g$ value measurements, in the range 120—294 K, but as the data of Mabbs and Porter [2] are measured at $Q$-band frequency, the measurements are not complicated by exchange coupling and are considered the more accurate,[27] although limited to only two temperatures. A single temperature measurement [28] of copper doped $[NH_4]_2[Zn(OH_2)_6][SO_4]_2$ at 20 K using single crystals yielded the $g$ values 2.46, 2.12, and 2.05. This clearly indicates a difference in the $g$ values for the copper doped potassium and ammonium Tutton salts and the highest and lowest $g$ values suggest that the $g$ values for the concentrated and doped ammonium Tutton salts are not significantly different, Figure 4. Unfortunately, the intermediate $g$ value of the doped ammonium Tutton salt, 2.12, is significantly higher than the corresponding extrapolated $g$ value for either of the concentrated $NH_4^+$ Tutton salt measurements. While this difference may be experimental, it may also be due to the co-operative Jahn–Teller effect.[22]

A linear extrapolation of the single-crystal [2] $g$ values of the complex $[NH_4]_2[Cu(OH_2)_6][SO_4]_2$ to 0 K yields $g_3 = 2.50$, $g_2 = 2.03$, and $g_1 = 2.07$, Figure 4, giving a $\Delta g$ value ($g_3 - g_2$) of 0.47, which yields a $\Delta E$ value of 168 $cm^{-1}$ from a least-squares fit of the Boltzmann distribution function. While the linear extrapolation of the $g$ values ($\Delta g = 0.47$) is unrealistic, it is also reasonable that $\Delta g$ will not vary by more than $0.47 \pm 0.07$ to yield a $\Delta E$ value of $168 \pm 40$ $cm^{-1}$. Considering the uncertainty in the crystallographic $\Delta E$ value of $160 \pm 20$ $cm^{-1}$, the measurements of the $\Delta E$ value for (1) from both temperature-variable crystallographic data and single-crystal e.s.r. spectra are considered to be reasonably consistent. They represent the best attempt to date to demonstrate the consistency of $\Delta E$ values measured by these two widely differing physical techniques.

*Electronic Spectra.*—The electronic spectra of the $NH_4^+$, K, and Rb complexes have been previously reported;[29] they show little change with the cation present, with bands at ~7 500, ~10 000, and 12 000 $cm^{-1}$, which is surprising in view of the substantial changes in tetragonality present, Table 5. Nevertheless, it should be remembered that the crystallographic data reflect a time-averaged structure due to the long time-scale of data collection (~1 s),[30] whereas the electronic spectra with a very much shorter lifetime of $10^{-15}$ s [30] relate to the extrema of the fluxional distortion, namely, the underlying static $CuO_6$ chromophore stereochemistry. Consequently, the electronic spectra relate to the underlying static stereochemistry (tetragonality, $T = 0.858$) and not to the time-averaged r.t. structure determined by $X$-ray crystallography. Thus in the series of Tutton salts, the electronic spectra should be very similar and the calculation of bonding parameters [such as a.o.m. (angular overlap method) coefficients] should relate to the underlying static stereochemistry and not to the time-averaged [29,31] r.t. crystal structure. Within this series of Tutton salt cation distortion isomers,[32] *small* differences in the geometry of the static $CuO_6$ chromophore will be present, due to the 'plasticity effect',[23] and will account for the small differences observed in the electronic energies.

## Acknowledgements

The authors acknowledge the award of Department of Education Studentships (to M. D. and A. M.), a Senior Demonstratorship (to S. T.), the Computer Bureau, U.C.C. for computing facilities, Professor G. M. Sheldrick, Dr. S. Motherwell, Dr. R. Roberts (Cambridge University), and Professor K. N. Trueblood (University of California) for the use of their programs, and the Microanalytical Section, U.C.C. for analysis.

## References

1 B. L. Silver and D. Getz, *J. Chem. Phys.*, 1974, **61**, 638.
2 F. E. Mabbs and J. K. Porter, *J. Inorg. Nucl. Chem.*, 1973, **35**, 3219.
3 H. Montgomery and E. C. Lingafelter, *Acta Crystallogr.*, 1966, **20**, 659.
4 G. M. Brown and R. Chibambaram, *Acta Crystallogr., Sect. B*, 1969, **25**, 676.
5 D. J. Robinson and C. H. L. Kennard, *Cryst. Struct. Commun.*, 1972, **1**, 185.
6 G. Smith, F. H. Moore, and C. H. L. Kennard, *Cryst. Struct. Commun.*, 1975, **4**, 407.
7 K. G. Shields and C. H. L. Kennard, *Cryst. Struct. Commun.*, 1972, **1**, 189.
8 K. G. Shields, J. J. van der Zee, and C. H. L. Kennard, *Cryst. Struct. Commun.*, 1972, **1**, 371.
9 M. Duggan, A. Murphy, and B. J. Hathaway, *Inorg. Nucl. Chem. Lett.*, 1979, **15**, 103.
10 N. W. Alcock, in 'Crystallographic Computing,' ed. F. Ahmed, Munksgaard, Copenhagen, 1970.
11 D. T. Cromer and D. Liberman, *J. Chem. Phys.*, 1970, **53**, 1891; D. T. Cromer and J. B. Mann, *Acta Crystallogr., Sect. A*, 1968, **24**, 321.
12 G. M. Sheldrick, SHELX 76, A Program for $X$-Ray Crystal Structure Determination, University of Cambridge, 1976.
13 K. N. Trueblood, THMI-1977, A Program for Rigid Body Analysis, University of California, 1977.

14 B. J. Hathaway and D. E. Billing, *Coord. Chem. Rev.*, 1970, **5**, 143.
15 B. J. Hathaway, M. Duggan, A. Murphy, J. Mullane, C. Power, A. Walsh, and B. Walsh, *Coord. Chem. Rev.*, 1981, **36**, 267.
16 A. W. Hewat and B. J. Hathaway, *J. Solid State Chem.*, in the press.
17 A. W. Hewat, Harwell Report 1973, No. 73/239 and ILL Report 74/H625; A. W. Hewat and I. Bailey, *Nucl. Instrum. Methods*, 1976, **137**, 463.
18 C. Simmons, A. Clearfield, W. Fitzgerald, S. Tyagi, and B. J. Hathaway, *Inorg. Chem.*, 1983, **22**, 2463.
19 J. D. Dunitz, ' *X*-Ray Analysis and the Structure of Organic Molecules,' Cornell University Press, Ithaca and London, 1979, p. 312.
20 C. Simmons, A. Clearfield, W. Fitzgerald, S. Tyagi, and B. J. Hathaway, *J. Chem. Soc., Chem. Commun.*, 1983, 189.
21 H. Montgomery and E. C. Lingafelter, *Acta Crystallogr.*, 1964, **17**, 1295.
22 D. Reinen and C. Friebel, *Struct. Bonding (Berlin)*, 1979, **37**, 1.
23 J. Gazo, I. B. Besuker, J. Garaj, M. Kabesova, J. Kohout, H. Langfelderova, M. Melnik, M. Seraton, and F. Valach, *Coord. Chem. Rev.*, 1976, **11**, 253.
24 J. H. Ammeter, H. G. Burgi, E. Gamp. V. Meyer-Sandrin, and W. P. Jensen, *Inorg. Chem.*, 1979, **18**, 733.
25 M. Duggan, B. J. Hathaway, and J. Mullane, *J. Chem. Soc., Dalton Trans.*, 1980, 690.
26 B. Walsh and B. J. Hathaway, *J. Chem. Soc., Dalton Trans.*, 1980, 681.
27 R. S. Drago, ' Physical Methods in Chemistry,' W. B. Saunders Co., Philadelphia, 1977, p. 317.
28 B. Bleaney, K. D. Bowers, and D. J. E. Ingram, *Proc. R. Soc. London, Ser. A*, 1955, **288**, 147.
29 R. C. Marshall and D. W. James, *J. Phys. Chem.*, 1974, **78**, 1235; M. A. Hitchman and T. D. Waite, *Inorg. Chem.*, 1976, **15**, 2150.
30 E. L. Muetterties, *Inorg. Chem.*, 1965, **4**, 795.
31 M. A. Hitchman and T. D. Waite, *Inorg. Chem.*, 1976, **15**, 2155.
32 L. Hulett, R. Sheahan, N. Ray, and B. J. Hathaway, *Inorg. Nucl. Chem. Lett.*, 1978, **14**, 305.

*Received* 24*th March* 1983; *Paper* 3/470